J Mater Sci (2017) 52:1617–1624

Blending PLLA/tannin-grafted PCL fiber membrane for skin tissue engineering

Suchen Jiang[1], Ping Song[1], Huiling Guo[1], Xue Zhang[1], Yajun Ren[1], Huanchao Liu[1], Xiaofeng Song[1,*], and Mingming Kong[1]

[1] *School of Chemical Engineering, Changchun University of Technology, Changchun 130012, People's Republic of China*

Received: 22 July 2016
Accepted: 28 September 2016
Published online: 13 October 2016

ABSTRACT

To create novel materials of skin tissue engineering, the blends of tannin-grafted poly(ε-caprolactone) (TA-*g*-PCL) and poly(L-lactic acid) (PLLA) have been prepared by electrospinning, and their corresponding characteristics are evaluated such as morphology, FTIR, thermodynamics, mechanics, wettability, as well as biocompatibility. TA-*g*-PCL and PLLA can be well blended to make smooth fibers, and fibrous diameter turns thinner with blending TA-*g*-PCL. At 15 wt%, the fibrous membrane shows higher tensile strength and elongation at a break than the other samples due to its best crystallinity. Membranous wettability drops with blending TA-*g*-PCL, but it increases sharply after incorporating PF108. At the same time, PLLA/TA-*g*-PCL fiber membrane is biocompatible. The biodegradable PLLA/TA-*g*-PLLA membrane is a promising candidate as skin tissue engineering.

Introduction

Electrospinning is an elegant and versatile method to produce fibrous membranes [1, 2]. The electrospun fibrous meshes are characterized with high surface-to-volume ratio and porosity which can mimic natural extracellular matrix (ECM) and thus promote cell adhesion, migration, and proliferation [3, 4]. Recently, electrospun aliphatic polyesters like poly(glycolic acid) (PGA), poly(L-lactic acid) (PLLA), their random copolymers poly(ε-caprolactone), and (PCL) have attracted a great deal of attention for drug delivery, surgical implantation, enzyme immobilization, tissue regeneration, as well as prevention of post-operative-induced adhesions [5–8]. Although the aliphatic polyesters are biodegradable and biocompatible, these polymeric fiber meshes are still not good enough to be applied in tissue engineering due to weak bioactivity.

To overcome the shortcoming, great efforts are contributed to develop the composite fibers of aliphatic polyesters and natural macromolecule via the electrospinning for better properties such as PLGA/chitosan [9, 10], PCL/gelatin [11], PLLA/keratin [12], and PLGA/collagen [13]. In addition, the modification of electrospun aliphatic polyester fibers using inorganic nanomaterials has been also investigated for applications in tissue engineering [14]. For example, antimicrobial fibers of PCL were prepared by electrospinning of a PCL solution with small

Address correspondence to E-mail: jlsongx@163.com

DOI 10.1007/s10853-016-0455-x

amounts of silver-loaded zirconium phosphate nanoparticles for wound dressing [15].

Tannin (TA) is a natural polyphenols containing polyphenolic group connected to a polyhydric alcohol core through ester linkages. It has recently attracted extensive research interesting due to diverse biological properties of TA including antioxidant antibacterial and anticarcinogenic [16–18] and its capability of interaction with proteins, which have been explored for biomedical applications such as skin [19–23]. Then biodegradable polyester fibers combining TA might be suitable as a scaffold with improved mechanical and biological properties. Recently, we have synthesized TA-grafted PCL via the ring-opening polymerized reaction. The dissolubility of TA in chloroform as well as compatibility with aliphatic polyesters was improved significantly [24].

In the current work, we blend PLLA with TA-*g*-PCL to produce the fiber membrane, and investigate into the effect of blending ratio of PLLA and TA-*g*-PCL on morphology, thermodynamics, mechanics, and wettability. Its cytotoxicity was also appreciated in vitro by MTT method. The obtained fiber mesh exhibits an attractive prospect in skin tissue engineering. To the best of our knowledge, this is the only example of combining biodegradable polyester and TA-*g*-PLLA via electrospinning.

Experimental

Materials

PLLA ($M_n = 75{,}871$) was purchased from Haizheng Biomaterials Co Ltd. Tannin ($M_n = 1300$) was procured form Shentong Science and Technology Co. Ltd. To improve the compatibility of tannin and PLLA, tannin-grafted PCL was also prepared in our lab [24]. Its number-average molecular weight was 3513. Other chemicals such as triethyl benzyl ammonium chloride (TEBAC), Pluronic F-108(PF-108), and chloroform were obtained commercially and used without further purification.

Preparation of electrospun fiber membranes

A certain amount of PLLA and dried TA-*g*-PCL were dissolved into chloroform to prepare a series of 7 wt% solutions. Their weight ratios were 90/10, 85/15, and 80/20, respectively. 1 wt% TEBAC with respect to the polymer was added into the above solutions to improve the electrospinning process. Preparation of 7 wt% PLLA solution was also served as a control.

The procedure of electrospun fiber mesh has been described previously [25]. The solution was put into a 5-ml syringe with a metal needle, which was installed on digital microinjection pump (Jiashan Ruichueng Eletranic Tec Co. Ltd, RSP01-B). The inner diameter of the orifice was 0.9 mm. 8 kV was provided between the cathode and anode by electrostatic generator (Gamma high voltage, USA) at a distance of 15–20 cm to prepare the fiber meshes. A steady flow of the solution from the orifice was controlled in 0.2 ml/min. The electrospinning was carried out under ambient conditions. The collected fiber membranes were vacuum drying at 30 °C for 24 h.

Chemical and physical characteristics of fibrous membranes

Electrospun fibrous morphologies were determined by an environmental scanning electron microscope (Model XL 30 ESEMFEG, Philips). A layer of gold was sprayed uniformly over the sample surfaces before the observation.

The chemical analysis of electrospun fibers was conducted by a Fourier transform infrared (FTIR) spectrometer (Nicolet iS10, Thermo Fisher Scientific) in the wavelength range between 400 and 4000 cm^{-1} using KBr pellets at ambient temperature.

Melting temperature (T_m) of various electrospun meshes were evaluated by differential scanning calorimetry (Perkin-Elmer DSC-7) [26]. The melting enthalpies (ΔH_m) of the samples were calculated from the fusion peaks in the first heating run of DSC curve. The samples were heated over a temperature range from −80 to 200 °C at a rate of 10 °C/min in a N_2 atmosphere.

Mechanics properties of electrospun meshes were measured on a tensile tester (YHS-229WG, Shanghai Yihuan Co. Ltd., China) at across-head speed of 5 mm/min at room temperature. All fiber meshes were processed into a rectangular shape with a dimension of 35 × 7.5 mm [2] and thickness of 0.2 mm. Both the tensile strength and elongation at a break were obtained from the stress–strain curves and were averaged over five samples.

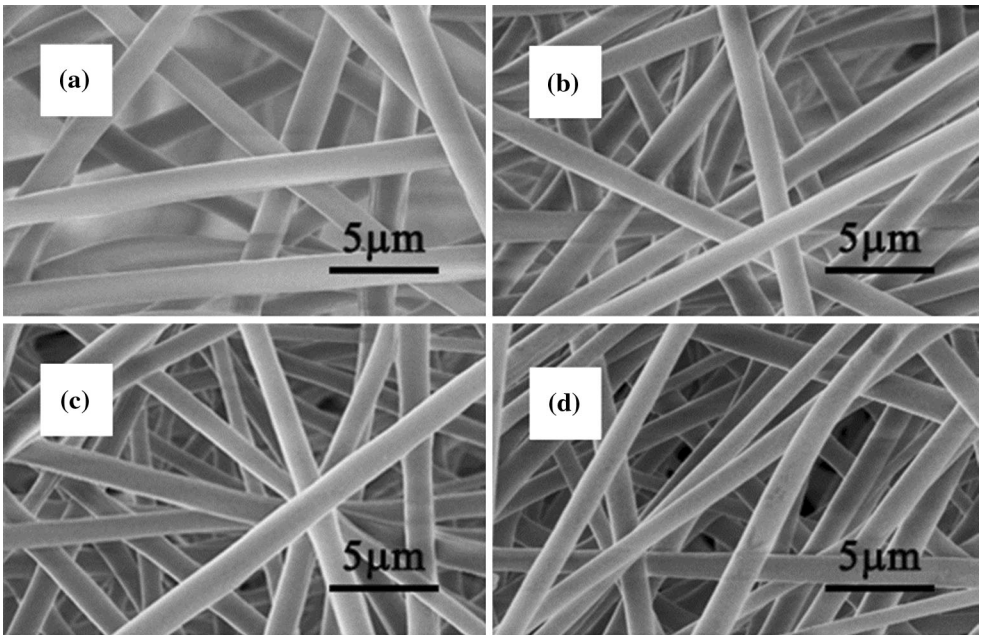

Figure 1 ESEM images of original PLLA fibers (**a**) and various composite fibers containing **b** 10 wt%, **c** 15 wt%, and **d** 20 wt% of TA-*g*-PCL with respect to PLLA.

Water contact angles indicating the wettability of the materials were appreciated by drop shape analysis (Beijing HARKE-SPCA, China) at 25 °C. The 1 × 1 cm [2] freshly prepared electrospun mesh was kept under vacuum for 24 h, and then every mesh was attached to a glass slide for contact angle measurements. A single droplet of doubly distilled water (2 μl) was applied to the mesh surface and contact angle was measured until equilibrium. Three measurements were done at different locations and the average value was obtained with standard deviation.

Cytotoxicity

Cytotoxicity of the material was examined by MTT assay (Roche, Germany) of cell viability [25]. Electrospun PLLA and TA-*g*-PCL/PLLA meshes were cut out with punch and put into 24-well culture plates. Cell culture fluid was used as negative control. Neonatal human dermal fibroblasts (NHDF, Cascade Biologics Incorporation) were seeded (7×10^3 cells/well) in 0.1 ml Dulbecco's Modified Eagle's Medium (DMEM) and then incubated at 37 °C in 5 % CO_2/air condition. Cell viability was monitored at 72 h by MTT assays and quantified using an ELISA reader.

Cell proliferation ratio (RGR) was calculated from RGR (%) = $OD_E/OD_C \times 100$ %, where OD_E was optical density that the detected group absorbed, and OD_C was optical density that the control group absorbed. And material toxicity was classified into five grades according to RGR as shown in Ref. [27] where levels 0 and 1 were non-toxic. OD was expressed as mean ± standard deviations of a representative of three similar experiments carried out in triplicate. Statistical analyses were performed with SPSS11.0 statistical software. Student–Newman–Keuls (SNK) was used to determine the significant differences among the groups, and α values less than 0.05 were considered significance.

Results and discussion

Microscopic evaluation

Figure 1 shows ESEM micrographs of original PLLA and various blending fibers containing 10, 15, and 20 wt% of TA-*g*-PCL with respect to PLLA. The blending fibers are smooth and uniform. Compared to the original PLLA fibers (1666.67 ± 155.25 nm), the average diameter of the blending fibers is slightly thinner, and decreases from 1458.33 ± 171.08 to 1382.36 ± 208.51, 1410.98 ± 131.63 nm with blending TA-*g*-PCL. It is well known that the fiber diameters will depend primarily on polymer concentration and

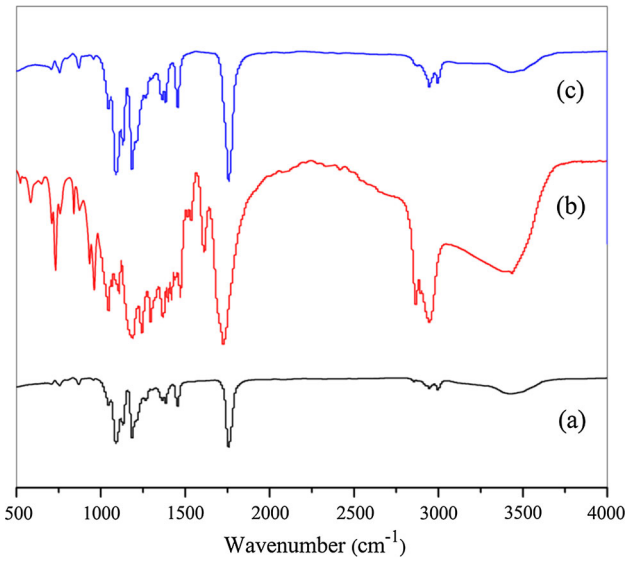

Figure 2 FTIR spectra of PLLA fibers (**a**), TA-*g*-PCL (**b**), and PLLA/15 % TA-*g*-PCL fibers (**c**).

applied voltage. The higher the polymer concentration, the larger the resulting nanofiber diameters will be [28]. A higher applied voltage ejects more fluid in a jet, resulting in a larger fiber diameter [29]. The two parameters are the same in this work, but PLLA content in fibers gradually drops, resulting in fibrous diameter decrease.

Chemical analysis

Figure 2 gives FTIR spectra of neat PLLA fibers, TA-*g*-PCL, and PLLA/15wt% TA-*g*-PCL composite fibers. The stretching vibration peaks of C=O and C–O in PLLA fibers individually hover around 1757 and 1088 cm^{-1}, while stretching and bending vibration of CH_3 appear at 1455 and 2995 cm^{-1} [30]. Compared to original PLLA fibers, the corresponding peaks of 15 wt% TA-*g*-PCL/PLLA composite fibers enhance significantly, but neither new peak nor peak shift appear in the composite fibers, indicating that the two components are physical blend together.

Thermodynamics analysis

To determine macromolecular aggregation in the fiber membranes, original PLLA and various PLLA/TA-*g*-PCL composite membranes were studied by DSC. The results are collected in Fig. 3 and Table 1. The melting (T_m) of PLLA can be clearly observed, and T_m drops from 172.10 °C for original PLLA fibrous membranes to 167.67–169.24 °C for the

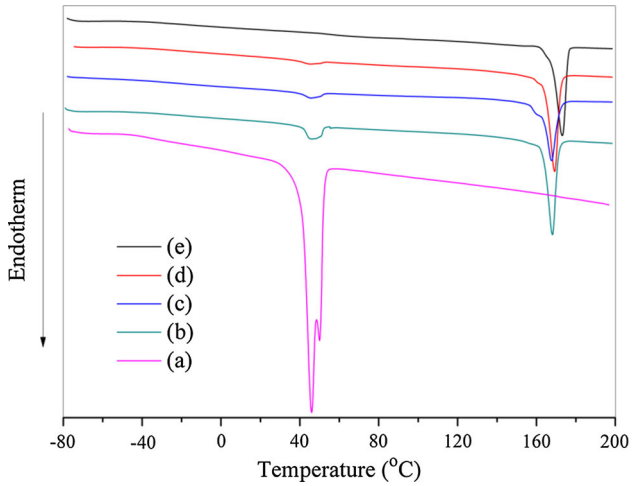

Figure 3 DSC curves of TA-*g*-PCL (**a**) and fibrous meshes containing 20 wt% (**b**), 15 wt% (**c**), 10 wt% (**d**), as well as 0 wt% (**e**) of TA-*g*-PCL.

composite meshes, suggesting that crystallization of PLLA could be subject to TA-*g*-PCL. Then degree of crystallinity (X_c) is further figured out according to the equation $X_c = (\Delta H_m/93.7\ J/g) \times 100\ \%$, where ΔH_m stands for the melting enthalpy in J/g that is calculated from the fusion peaks in the first heating run of DSC curve, and 93.7 J/g is the specific enthalpy of melting for 100 % crystalline PLLA [26]. It can be found that X_c decreases from original 48.3 to 47.5 % with the blend of 10 wt% TA-*g*-PLLA into PLLA. However, a dramatic scene occurs with the content of TA-*g*-PCL increasing further. X_c climbs to the maximum (50.3 %) at 15 wt% of TA-*g*-PCL, while it hits rock bottom (42.6 %) at 20 wt%.

When a small amount of TA-*g*-PCL is blended into PLLA, hydrogen bonds which could form between TA-*g*-PLLA and PLLA prevent PLLA molecular chain from folding and rearranging, resulting in a decrease of PLLA crystal. As shown in Fig. 3, TA-*g*-PCL can form a little of imperfect crystals at low temperature with its content increasing to 15 wt%, and these crystals serve as heterogeneous nucleation

Table 1 DSC data of various fibrous meshes

Fiber meshes	T_m (°C)	ΔH_m (J/g)	X_c*(%)
PLLA	172.10	45.25	48.3
10 % TA-*g*-PCL/PLLA	169.24	44.55	47.5
15 % TA-*g*-PCL/PLLA	167.67	47.17	50.3
20 % TA-*g*-PCL/PLLA	168.13	39.92	42.6

* $X_c = \Delta H_m/93.7\ J/g \times 100\ \%$

to facilitate crystallization of PLLA [31]. As the amount of TA-*g*-PCL in the fibrous membrane is 20 wt%, distinct melting peak corresponded to pure TA-*g*-PCL show that it can assemble into the larger crystal structure which inhibits PLLA crystal from growing.

Mechanics properties

Considering a desirable guided tissue regeneration scaffold is characterized with mechanical stability and good manageability [32], tensile testing has been carried out to check the effect of the addition of TA-*g*-PCL on the mechanical property such as tensile stress and elongation at break. Figure 4 shows the relationships between membranous tensile properties and TA-*g*-PCL blending content. The tensile strength of PLLA/TA-*g*-PCL samples reaches a maximum at 15 wt% blending, which is 4.32 ± 0.33 MPa, then dropped swiftly to 2.20 ± 0.22 MPa with the blending content increasing to 20 wt%. Tensile properties of electrospun fiber membrane are dependent on multiple factors like polymeric crystallinity, intermolecular interaction [25], as well as molecular structure. On the one hand, stiffness of tannic molecule is high due to its aromatic architecture, and on the other, the mobility of PLLA molecular tangled with PCL is also restricted because the brachial PCL is bound by the central tannic core. So blending TA-*g*-PCL improves the membranous tensile strength. However, when the blending content is more than 15 wt%, TA-*g*-PCL which begins agglomeration brings about the crystallinity decrease of PLLA matrix. Then the membranous tensile strength

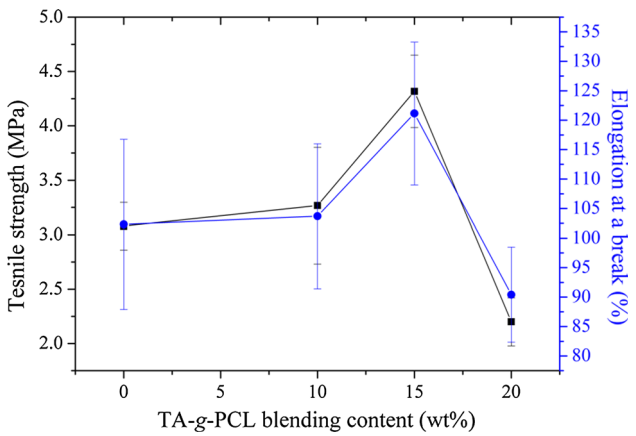

Figure 4 TA-*g*-PCL blending content in PLLA fibrous membranes versus **a** tensile strength and **b** elongation at break.

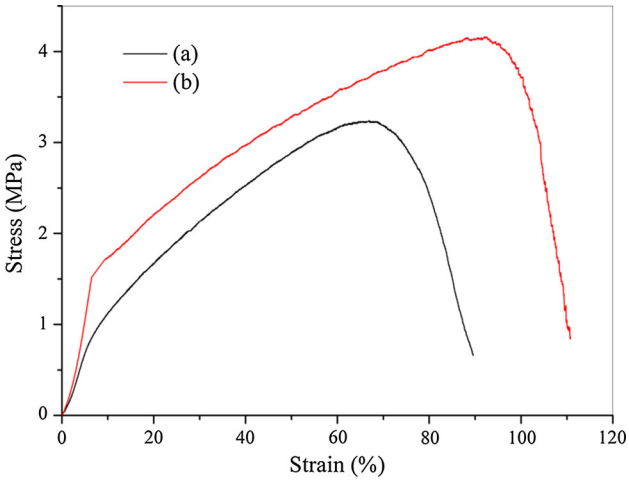

Figure 5 Stress–strain curves of **a** original PLLA and **b** PLLA/15 wt% TA-*g*-PCL fibrous membrane.

declines. As shown in Fig. 4, elongation at break also appears the similar trend, and is the best 121.14 ± 12.13 % at 15 wt% blending.

Stress–strain curves of original PLLA and PLLA/15 %TA-*g*-PCL blending membrane are also presented in Fig. 5. The stress of original and blending membrane initially shows a linear increase with strain going up, and non-linearity increase appears at around 10 % strain. Then their Young's modulus values are 55.2 ± 6.2 MPa and 93.0 ± 12.3 MPa, respectively. Moreover, the strain at the failure increased from 67 to 97 % with the addition of TA-*g*-PLLA into PLLA matrix. It is visible that appropriate

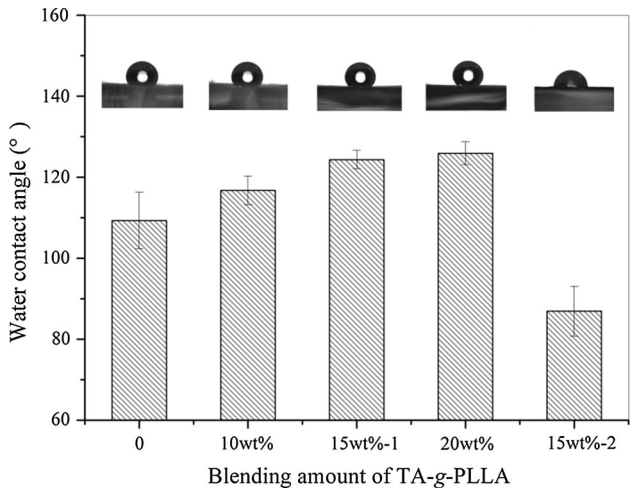

Figure 6 TA-*g*-PCL blending content in the fibrous membranes versus contact angle; the upper photographs are water droplets on the corresponding fibrous membranes; "15 wt%-1" and "15 wt%-2" stand for the membranes with and without PF-108, respectively.

Table 2 In vitro cytotoxicity of different samples toward NHDF cells after incubation for 72 h

Group	OD*	RGR (%)	Grade
Original PLLA fibrous mesh	0.75263 ± 0.00172	91.55	1
15 wt% TA-*g*-PCL/PLLA fibrous mesh	0.78024 ± 0.00155	88.31	1
Control	0.85223 ± 0.00167	100.0	0

* Data were presented as mean standard deviation ($n = 3$)

blending TA-*g*-PLLA not only enhances membranous mechanical stability but also improves significantly toughness. In application of tissue engineering, a perfect scaffold should provide necessary mechanical support to assume cell and new tissue formation [32].

Wettability

Water contact angle measurement data of different fibrous membranes are compiled in Fig. 6, where contact angle turns large by increasing TA-*g*-PCL content in the fiber membranes. Contact angle of original PLLA fiber mesh is 109.28 ± 6.07°, while that of 20 wt% TA-*g*-PLLA/PLGA fiber mesh increase to 125.89 ± 2.83°. The upper photographs in Fig. 6 further display that water droplets on the surface of mesh seem to trend circular shape with the increase of TA-*g*-PCL content in PLLA matrix. This results from the decrease of hydroxyl group in TA molecules and the incorporation of hydrophobic PCL molecular chain, and it has been found in a previous work that the water contact angle of the fibrous membrane increases significantly when six-armed PCL is blended into PLGA [33]. Nevertheless, it is well known that wettability of electrospun fiber membrane can be easily modified through multiple methods such as chemical treatment [34], high-energy radiation treatment [35], and blending [34] and copolymerization of hydrophilic polymers [9]. As shown in Fig. 6, water contact angle drops from 124.32 ± 2.29° to 86.93 ± 6.14° when 1 wt% PF108 is added to the blending membrane. Due to the hydrophobic interaction between the $-CH_3$ groups of polymer and the $-CH_3$ groups of PF-108, it restricts the integration of EO segments of PF108 into the polymer chains and hence projects them toward the fibrous surface [33].

In vitro cytotoxicity

As a potential scaffold for tissue engineering, the fibrous matrix should exhibit cytocompatibility. Cytotoxicity tests from MTT assays of cell viability in fibrous matrix were studied. *RGR* was figured out on the basis of the negative control group, and the result is shown in Table 2. The *RGR*s of the original PLLA and the blending PLLA/TA-*g*-PCL membrane, 91.55 and 88.31 %, respectively, differ slightly, but they are of level 1 toxicity. In other words, both fibrous membranes have no signs of cytotoxicity. Then PLLA/TA-*g*-PCL fiber membrane with good biocompatibility qualified as tissue engineering scaffold.

Conclusions

In the work, we firstly prepared PLLA/TA-*g*-PCL fibrous membrane for skin tissue engineering. The blends are investigated in detail such as morphology, chemical structure, thermodynamics, mechanics, wettability, as well as biocompatibility. The results show that TA-*g*-PCL and PLLA can be well blended to make smooth fibers, and fibrous diameter gradually decreases from 1666.67 to 1382.36 nm with blending TA-*g*-PCL. The two components are only blended physically. The fibrous membrane with 15 wt% of TA-*g*-PCL shows higher tensile strength and elongation at a break compared to the other samples due to its best crystallinity. Although membranous wettability decreases with blending TA-*g*-PCL, it improves obviously after incorporating 1 wt% PF108. At the same time, PLLA/TA-*g*-PCL fiber membrane is not cytotoxic. In order to better serve skin tissue engineering, designs of a more prefect membrane are undertaken.

Acknowledgements

This work was supported by the project of Science and Technology bureau of Changchun (Grant No. 14KG106); Education Department of Jilin (Grant No. 2014123); and the Natural Science Foundation of Jilin province (Grant No. 20130102065JC).

References

[1] Agarwal S, Wendorff JH, Greiner A (2008) Use of electrospinning technique for biomedical applications. Polymer 49:5603–5621

[2] Wang ZG, Wan LS, Liu ZM, Huang XJ, Xu ZK (2009) Enzyme immobilization on electrospun polymer nanofibers: an overview. J Mol Catal B 56:189–195

[3] Smith LA, Ma PX (2004) Nano-fibrous scaffolds for tissue engineering. Colloid Surf B 39:125–131

[4] Li WJ, Laurencin CT, Caterson EJ, Tuan RS, Ko FK (2002) Electrospun nanofibrous structure: a novel scaffold for tissue engineering. J Biomed Mater Res 60:613–621

[5] Zeng J, Xu X, Chen X, Liang Q, Bian X, Yang L, Jing X (2003) Biodegradable electrospun fibers for drug delivery. J Control Release 92(3):227–231

[6] Zong X, Ran S, Fang D, Hsiao BS, Chu B (2003) Control of structure, morphology and property in electrospun poly(glycolide-*co*-lactide) non-woven membranes via post-draw treatments. Polymer 44(17):4959–4967

[7] Zeng J, Chen X, Liang Q, Xu X, Jing X (2004) Enzymatic degradation of poly(L-lactide) and poly(ε-caprolactone) electrospun fibers. Macromol Biosci 4(12):1118–1125

[8] Kim K, Luu YK, Chang C, Fang D, Hsiao BS, Chu B, Hadjiargyrou M (2004) Incorporation and controlled release of a hydrophilic antibiotic using poly(lactide-*co*-glycolide)-based electrospun nanofibrous scaffolds. J Control Release 98(1):47–56

[9] Li AD, Sun ZZ, Zhou M, Xu XX, Ma JY, Zheng W, Zhou HM, Li L, Zheng YF (2013) Electrospun Chitosan-graft-PLGA nanofibres with significantly enhanced hydrophilicity and improved mechanical property. Colloids Surf B 102:674–681

[10] Meng ZX, Zheng W, Li L, Zheng YF (2011) Fabrication, characterization and in vitro drug release behavior of electrospun PLGA/chitosan nanofibrous scaffold. Mater Chem Phys 125(3):606–611

[11] Chong EJ, Phan TT, Lim IJ, Zhang YZ, Bay BH, Ramakrishna S, Lim CT (2007) Evaluation of electrospun PCL/gelatin nanofibrous scaffold for wound healing and layered dermal reconstitution. Acta Biomater 3(3):321–330

[12] Li JS, Li Y, Li L, Mak AFT, Ko F, Qin L (2009) Preparation and biodegradation of electrospun PLLA/keratin nonwoven fibrous membrane. Polym Degrad Stab 94:1800–1807

[13] Jose MV, Thomas V, Dean DR, Nyairo E (2009) Fabrication and characterization of aligned nanofibrous PLGA/Collagen blends as bone tissue scaffolds. Polymer 50:3778–3785

[14] Meng ZX, Zheng W, Li L, Zheng YF (2010) Fabrication and characterization of three-dimensional nanofiber membrance of PCL–MWCNTs by electrospinning. Mater Sci Eng 30:1014–1021

[15] Duan UY, Jia J, Wang SH, Yan W, Jin L, Wang ZY (2007) Preparation of antimicrobial poly(ε-caprolactone) electrospun nanofibers containing silver-loaded zirconium phosphate nanoparticles. J Appl Polym Sci 106(2):1208–1214

[16] Chen KS, Hsiao YC, Kuo DY, Choua MC, Chud SC, Hsieh YS, Lin TH (2009) Tannic acid-induced apoptosis and -enhanced sensitivity to arsenic trioxide in human leukemia HL-60 cells. Leuk Res 33(2):297–307

[17] Sakagami H, Jiang Y, Kusama K, Atsumi T, Ueha T, Toguchi M, Iwakura I, Satoh K, Ito H, Hatano T, Yoshida T (2000) Cytotoxic activity of hydrolyzable tannins against human oral tumor cell lines—a possible mechanism. Phytomedicine 7(1):39–47

[18] Tikoo K, Sane MS, Gupta C (2011) Tannic acid ameliorates doxorubicin-induced cardiotoxicity and potentiates its anticancer activity: potential role of tannins in cancer chemotherapy. Toxicol Appl Pharmacol 251(3):191–200

[19] Kozlovskaya V, Zavgorodnya O, Chen Y, Ellis K, Tse HM, Cui W, Thompson JA, Kharlampieva E (2012) Ultrathin polymeric coatings based on hydrogen-bonded polyphenol for protection of pancreatic islet cells. Adv Funct Mater 22(16):3389–3398

[20] Chen J, Kozlovskaya V, Goins A, Campos-Gomez J, Saeed M, Kharlampieva E (2013) Biocompatible shaped particles from dried multilayer polymer capsules. Biomacromolecules 14(11):3830–3841

[21] Dierendonck M, Fierens K, De Rycke R, Lybaert L, Maji S, Zhang Z, Zhang Q, Hoogenboom R, Lambrecht BN, Grooten J, Remon JP, De Koker S, De Geest B (2014) Nanoporous hydrogen bonded polymeric microparticles: facile and economic production of cross presentation promoting vaccine carriers. Adv Funct Mater 24(29):4634–4644

[22] Park JH, Yang SH, Lee J, Ko EH, Hong D, Choi IS (2014) Nanocoating of single cells: from maintenance of cell viability to manipulation of cellular activities. Adv Mater 26(13):2001–2010

[23] Zhuk I, Jariwala F, Attygalle AB, Wu Y, Libera MR, Sukhishvili SA (2014) Self-defensive layer-by-Layer films with bacteria-triggered antibiotic release. ACS Nano 8(8):7733–7745

[24] Song P, Jiang SC, Ren YJ, Zhang X, Qiao TK, Song XF, Liu QM, Chen XS (2016) Synthesis and characterization of tannin grafted polycaprolactone. J Colloid Interface Sci 479:160–164

[25] Li HT, Qiao TK, Song P, Guo HL, Song XF, Zhang BC, Chen XS (2015) Star-shaped PCL/PLLA blended fiber membrane via electrospinning. J Biomater Sci Polym Ed 26(7):420–432

[26] Qiao TK, Song P, Guo HL, Song XF, Zhang BC, Chen XS (2016) Reinforced electrospun PLLA fiber membrane via chemical crosslinking. Eur Polym J 74:101–108

[27] Zhou H, Du T, Shen Y, Wang Z, Zheng Y, Haapasalo M (2015) In vitro cytotoxicity of calcium silicate-containing endodontic sealers. J Endod 41:56–61

[28] Deitzel JM, Kleinmeyer J, Harris D, Tan NCB (2001) The effect of processing variables on the morphology of electrospun nanofibers and textiles. Polymer 42:261–272

[29] Demir MM, Yilgor I, Yilgor E, Erman B (2002) Electrospinning of polyurethane fibers. Polymer 43:3303–3309

[30] Prabhakaran MP, Venugopal J, Ramakrishna S (2009) Electrospun nanostructured scaffolds for bone tissue engineering. Acta Biomater 5:2884–2893

[31] Dell'Erba R, Groeninckx G, Maglio G, Malinconico M, Migliozzi A (2001) Immiscible polymer blends of semicrystalline biocompatible components: thermal properties and phase morphology analysis of PLLA/PCL blends. Polymer 42(18):7831–7840

[32] Jaiswal AK, Chhabra H, Soni VP, Bellare JR (2013) Enhanced mechanical strength and biocompatibility of electrospun polycaprolactone–gelatin scaffold with surface deposited nano-hydroxyapatite. Mater Sci Eng 33:2376–2385

[33] Li HT, Song P, Qiao TK, Cui QQ, Song XF, Zhang BC (2016) A quaternary composite fiber membrane for guided tissue regeneration. Polym Adv Technol 27(2):178–184

[34] Khang G, Choee JH, Rhee JM, Lee HB (2002) Interaction of different types of cells on physicochemically treated poly(L-lactide-*co*-glycolide) surfaces. J Appl Polym Sci 85:1253–1262

[35] Yoo HS, Kim TG, Park TG (2009) Surface-functionalized electrospun nanofibers for tissue engineering and drug delivery. Adv Drug Deliv Rev 61:1033–1042